Printed ethyl cellulose/$CuInSe_2$ composite light absorber layer and its photovoltaic effect

2011 J. Phys. D: Appl. Phys. 44 455401

(http://iopscience.iop.org/0022-3727/44/45/455401)

J. Phys. D: Appl. Phys. **44** (2011) 455401 (6pp) doi:10.1088/0022-3727/44/45/455401

Printed ethyl cellulose/$CuInSe_2$ composite light absorber layer and its photovoltaic effect

Qinmiao Chen[1,2], Xiaoming Dou[1,2,3], Zhenqing Li[1,2], Shuyi Cheng[2] and Songlin Zhuang[2]

[1] Department of Physics, Shanghai Jiao Tong University, 800 Dongchuan Road, Minhang District, Shanghai 200240, People's Republic of China
[2] Institute of Optical-Electrical Engineering, University of Shanghai for Science and Technology, 516 Jungong Road, Shanghai 200093, People's Republic of China
[3] Consolidated Research Institute for Advanced Science and Medical Care, Waseda University, 513 Wasedatsurumaki-cho, Shinjuku-ku, Tokyo 162-0041, Japan

E-mail: xm.dou@yahoo.com.cn

Received 1 August 2011, in final form 26 September 2011
Published 27 October 2011
Online at stacks.iop.org/JPhysD/44/455401

Abstract
A novel ethyl cellulose/$CuInSe_2$ (CISe) composite light absorber layer and its photovoltaic effect are reported. The precursor absorber layer was deposited from screen printing paste containing ethyl cellulose and CISe powder, and was followed by rapid thermal annealing. Experimental results indicated that the ethyl cellulose remained in the annealed absorber layer, and the composite absorber layer may consist of ethyl cellulose/CISe composite shell/core structure. The structural, optical and electronic properties of the composite absorber layer were fully investigated. The composite absorber layer shows photovoltaic efficiency of 0.65% under standard test condition.

(Some figures may appear in colour only in the online journal)

1. Introduction

Thin film chalcopyrite materials, such as $CuInSe_2$ (CISe) and its alloys with gallium and sulfur $CuIn_xGa_{1-x}(S,Se)_2$ (CIGS), have attracted much attention as solar cell absorber layer because of their large absorption coefficient ($10^5\ cm^{-1}$), high stability and demonstrated high solar cell conversion efficiency [1–3]. However, the absorber layers of high efficiency solar cells are usually prepared by vacuum processes, which are rather expensive, complicated and difficult to scale-up for commercial production. Consequently, many low-cost non-vacuum technologies, such as printing (screen printing, doctor blade, curtain coating, etc) [4–7], spin coating [8, 9], spraying pyrolysis [10] and electrochemical deposition [11, 12], have been developed recently as alternatives for the preparation of solar cell absorber layer.

Among these non-vacuum technologies, solution-based printing technology is a very promising technology for the fabrication of low-cost absorber layer due to its important advantages, e.g., simple, low-temperature, high material utilization efficiency (close to 100%) and compatibility with production process of high throughput roll-to-roll. In the printing process, polymer viscosity controlling agent is usually required to add into the printing paste, otherwise the coated paste cannot be fixed and will flow to the non-coated area. Ethyl cellulose, a frequently used polymer viscosity controlling agent, has been studied for the preparation of CIGS paste [5, 6, 13–15]. On the other hand, however, the employed ethyl cellulose may remain in the final absorber layer as amorphous carbon material after the annealing process [5, 15]. Moreover, the morphology and effect of the remained amorphous material have not been clearly understood till now [5, 14], which requires extended research.

In this study, a novel ethyl cellulose/CISe composite absorber layer is reported. CISe powder was applied as raw material and was dispersed by ethyl cellulose to prepare screen printing paste. The printed absorber layer was annealed in N_2 ambience by rapid thermal annealing (RTA). Experimental results indicated that the ethyl cellulose remained in the annealed absorber layer, and the composite absorber layer may

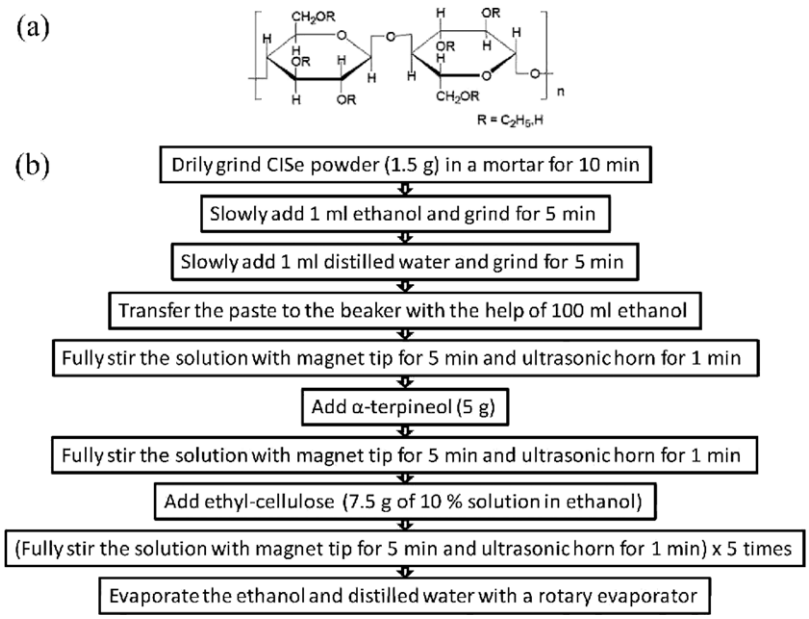

Figure 1. (*a*) Molecular structure of the ethyl cellulose; (*b*) Preparation scheme of the screen printing paste.

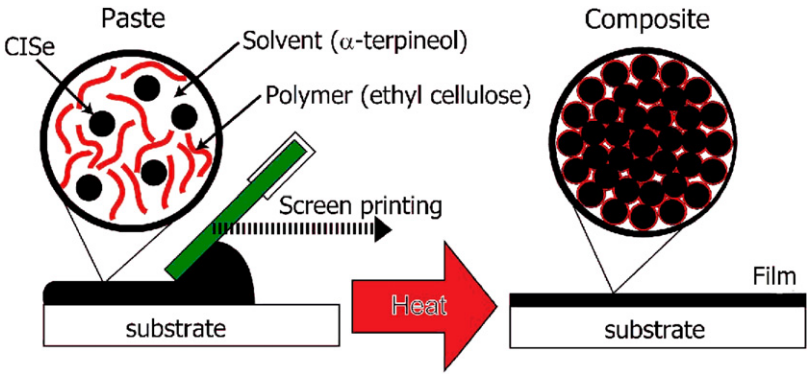

Figure 2. Schematic diagram of the ethyl cellulose/CISe composite absorber layer preparation process.

consist of ethyl cellulose/CISe composite shell/core structure. The annealing effects on the structural, optical and electronic properties of the composite absorber layer were studied.

2. Experimental method

2.1. Preparation of ethyl cellulose/CISe composite absorber layer

2.1.1. Synthesis of CISe powder. A simple ball milling process was applied for the synthesis of CISe powder. Element powders copper (Cu, 99.9%), indium (In, 99.99%) and selenium (Se, 99.9%) were mixed in molar ratio 1 : 1 : 2. The ball milling process was conducted by the planetary ball miller at various rotation speeds for 30 min to obtain single phase CISe powder. A rotation speed of 700 rpm was optimized for this purpose.

2.1.2. Preparation of screen printing paste. Ethyl cellulose was used as polymer viscosity controlling agent for the preparation of CISe paste, and its molecular structure is shown in figure 1(*a*). The preparation scheme of the screen printing paste is described in figure 1(*b*). Briefly, the CISe powder was homogeneously dispersed in solvent α-terpineol and polymer viscosity controlling agent ethyl cellulose to prepare printable paste.

2.1.3. Deposition of ethyl cellulose/CISe composite absorber layer. Paste was deposited on glass substrate by the screen printing method. After being dried at 125 °C for 5 min in air (dried sample was referred as 'as-deposited'), the sample was annealed in N_2 ambience by the RTA process at 600 °C for 15 min. A schematic diagram of the ethyl cellulose/CISe composite absorber layer preparation process is depicted in figure 2.

2.2. Characterization of ethyl cellulose/CISe composite absorber layer

Morphology of the absorber layer was observed by scanning electron microscope (SEM; JSM-6510, JEOL). Organic components were analysed by Fourier transform infrared

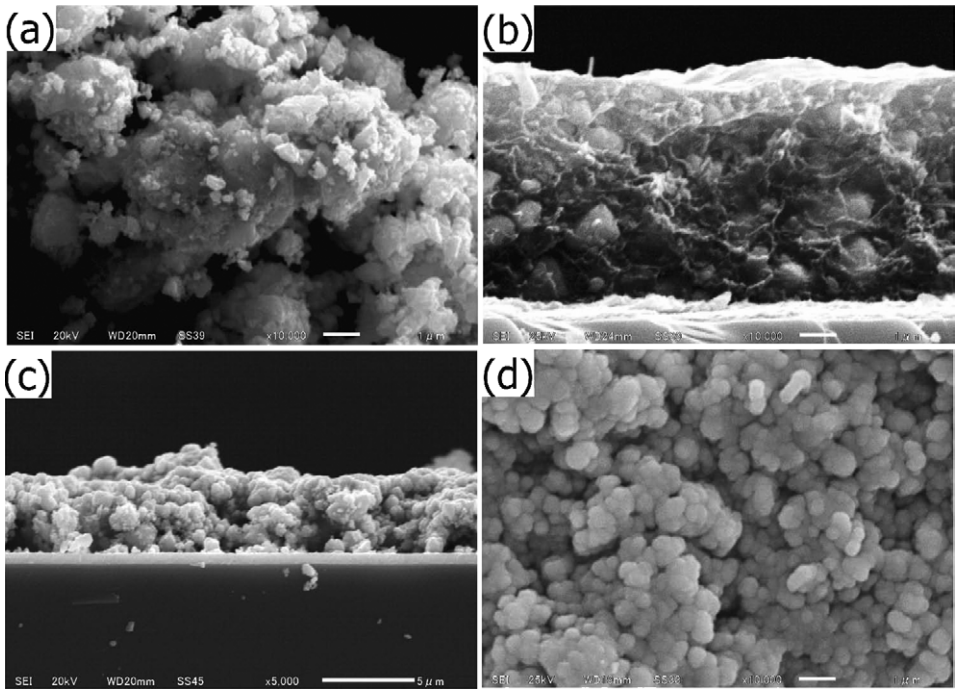

Figure 3. SEM (*a*) image of CISe powder; (*b*) cross-section image of an as-deposited absorber layer; (*c*) cross-section image of an annealed absorber layer; (*d*) surface image of an annealed absorber layer.

spectroscopy (FTIR; FT/IR-4200, JASCO). Crystallinity and phase composition were confirmed by x-ray diffraction spectrometer (XRD; MiniFlex, Rigaku). UV–vis–IR absorption spectra were measured in absorbance spectroscopy by spectrophotometer (Lambda 750, Perkin-Elmer).

In order to study the photovoltaic property of the absorber layer, a simple superstrate solar cell structure of Mo/absorber layer/In_2S_3/TiO_2/FTO glass was employed. Both compact TiO_2 window layer and In_2S_3 buffer layer were prepared by the spray pyrolysis method [16, 17], and their thicknesses were about 100 nm and 300 nm, respectively. Mo electrode was deposited by rf-sputtering. The active area of the solar cell is 0.5 cm × 0.5 cm. Photovoltaic measurement of the completed solar cell was performed under an AM 1.5 solar simulator equipped with a xenon lamp (YSS-100A, Yamashita Denso). The power of the simulated light was calibrated to 100 mW cm^{-2} using a reference Si photodiode (Bunkou Keiki). *J*–*V* (short-circuit current density J_{sc} and open-circuit voltage V_{oc}) curves were obtained by applying an external bias to the cell and measuring the generated photocurrent with an APCMT 6240 DC voltage current source.

3. Results and discussion

3.1. As-deposited absorber layer

Figure 3(*a*) shows the morphology of the CISe powder obtained by the ball milling process. The particle size of the powder is around 150–300 nm. Some small particles aggregated into big ones or clusters with diameter around 2–3 μm. Figure 3(*b*) describes the cross-section image of an as-deposited absorber layer. As shown in figure 3(*b*), the as-deposited absorber layer contains a large amount of viscosity controlling agent, and the CISe powder is embedded in. A typical XRD pattern of the as-deposited absorber layer is depicted in figure 4(*a*). The diffraction peaks are clearly observed at the positions of 26.72°, 44.22°, 52.48°, 64.58° and 70.88°, and can be assigned to CISe (1 1 2), (2 2 0)/(2 4 0), (3 1 2), (4 0 0) and (3 2 5) (PCPDF#872265), respectively. However, all the peaks are weak and broad, which may be caused by the poor crystallinity of the as-synthesized CISe powder and the large amount of viscosity controlling agent (causing the concentration of the CISe powder to be very low). Figure 5 shows the UV–vis–IR absorption spectrum of the as-deposited absorber layer. Because of the poor crystallinity of the CISe powder and the large amount of viscosity controlling agent, the absorption edge of the as-deposited absorber layer is not clear, and the light absorption is also not large in the UV–vis–NIR range in comparison with that of the annealed samples.

3.2. Ethyl cellulose/CISe composite absorber layer

Figure 3(*c*) shows the cross-section image of an annealed absorber layer. As can be seen from figure 3(*c*), the annealed absorber layer is a one-layer structure which is different from the previously reported double-layer structure [5, 15]. In previous contributions where metal salts were used as raw material for the preparation of printing paste, it was believed that the reaction of the raw materials with Se vapour during the selenium ambience annealing process was from top to bottom. Therefore, when a dense absorber layer was first formed on the top, the evaporation of the ethyl cellulose was hindered and sequentially the reaction between the metal salts and the Se vapour was stopped, inducing a double-layer structure with top dense absorber layer and bottom amorphous

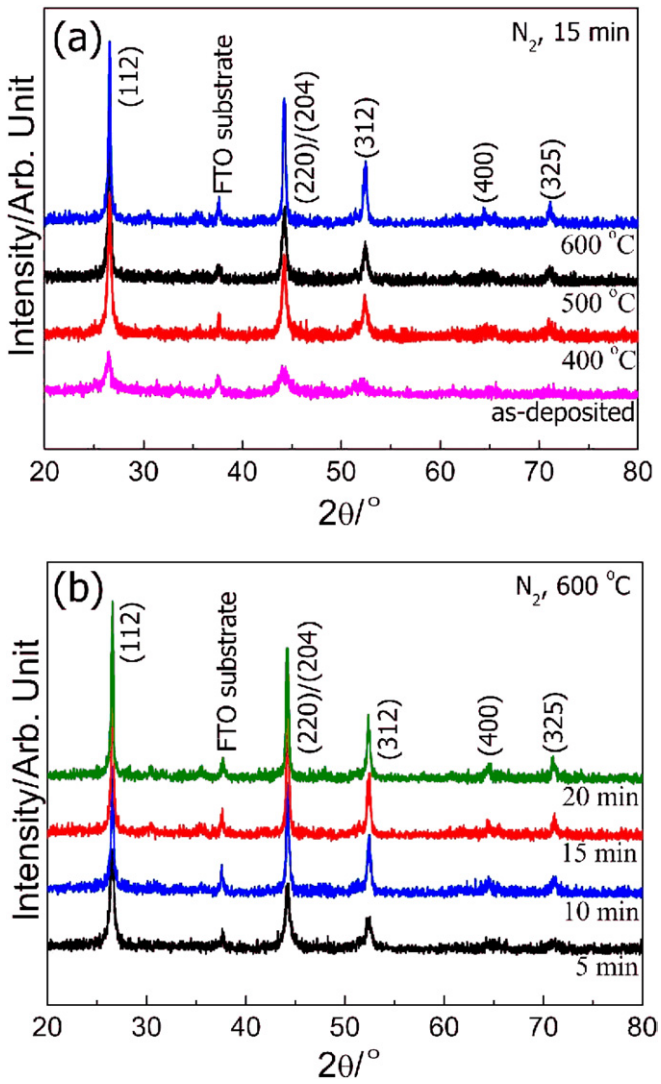

Figure 4. XRD patterns of composite absorber layers prepared at (*a*) various temperatures and (*b*) various times.

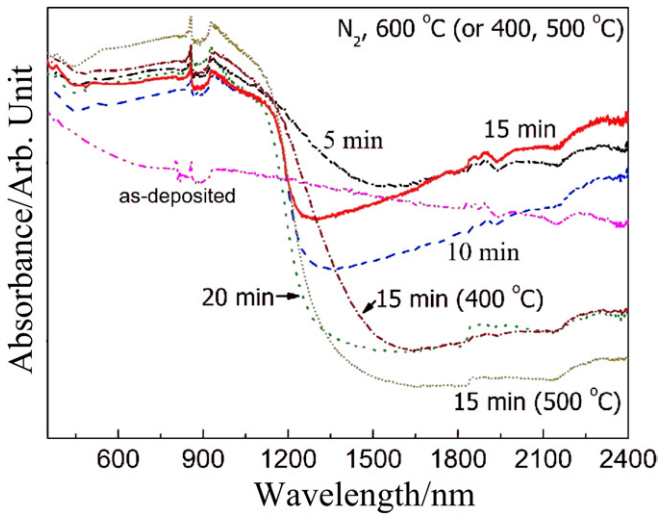

Figure 5. UV–vis–IR absorption spectra of composite absorber layers prepared under various conditions.

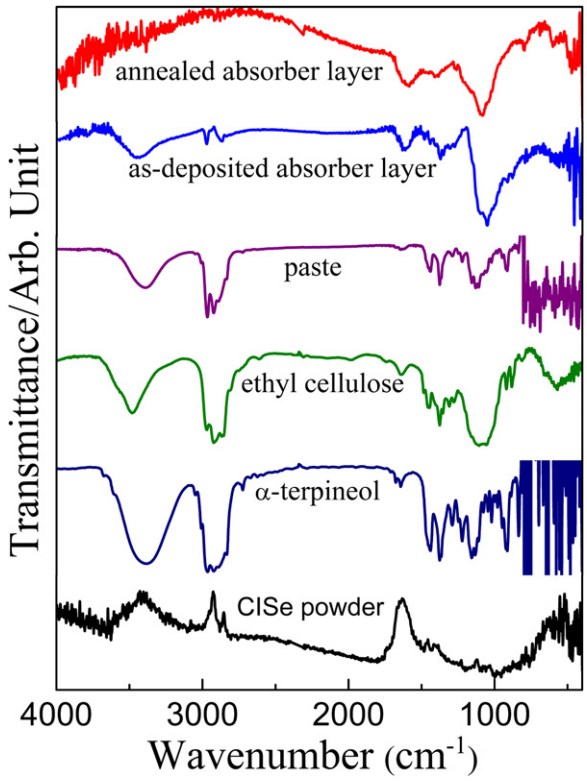

Figure 6. FTIR data of related samples.

carbon layer. While, in this study, the CISe powder was used to replace the metal salts as raw material, thus there is no chemical reaction during the annealing process. In addition, the particle size of the CISe powder is rather big, which also makes the evaporation of the viscosity controlling agent more easily. Therefore, in the annealed absorber layer, no separated amorphous carbon layer is observed. Furthermore, as observed in figures 3(*c*) and (*d*), there is also no visible viscosity controlling agent remaining in the annealed absorber layer.

To further identify whether there is viscosity controlling agent remaining in the annealed absorber layer, FTIR measurements of the related samples were carried out. As shown in figure 6, the peak intensity of the as-deposited absorber layer at the position of 2974 cm^{-1} becomes weaker compared with that of paste containing both solvent α-terpineol and polymer viscosity controlling agent ethyl cellulose, which may be due to the considerable evaporation of solvent α-terpineol by the drying treatment process (boiling point of the α-terpineol is around 219 °C [18]). The annealed absorber layer shows two peaks at the position of 1079 cm^{-1} and 1596 cm^{-1}. The peak at 1079 cm^{-1} is in the same position of ethyl cellulose, so this peak could come from the ethyl cellulose remaining in the annealed absorber layer. There should be no peaks from α-terpineol in the high-temperature annealed absorber layer since the boiling point of the α-terpineol is low. Therefore, the other peak at 1596 cm^{-1} may be of an amorphous carbon material being formed from the decomposition of ethyl cellulose at high temperature. The intensity of the peak at 1596 cm^{-1} is much weaker than that of 1079 cm^{-1}, thus the main component of the remaining

amorphous material could be ethyl cellulose (to simplify the description, the remaining amorphous material is referred as ethyl cellulose).

As a result, the annealed absorber layer does contain ethyl cellulose but the amount should be very small (as shown in figures 3(*c*) and (*d*), there is no visible viscosity controlling agent in the annealed absorber layer). In addition, the annealed absorber layer is a homogeneous film as observed in the SEM images. Therefore, we speculate that there is a high possibility that the ethyl cellulose/CISe composite absorber layer consists of ethyl cellulose/CISe shell/core structure (see figure 2, right).

3.3. Annealing effects on the properties of the ethyl cellulose/CISe composite absorber layer

In order to study the annealing effects on the structural, optical and electronic properties of the composite absorber layer, the as-deposited absorber layer was annealed in N_2 ambience by the RTA process under various conditions.

3.3.1. XRD analysis. To confirm the crystallinity and phase composition of the ethyl cellulose/CISe composite absorber layer, XRD measurements were performed. Figure 4(*a*) depicts the XRD pattern of samples annealed at various temperatures. As illustrated in figure 4(*a*), the XRD peaks of the annealed samples become sharp and strong in comparison with that of the as-deposited sample. The sharp and strong peak may be attributed to the improved micro-structural and macro-morphologic properties of the ethyl cellulose/CISe composite absorber layer. The crystallinity of the CISe was promoted by the annealing process. The amount of the ethyl cellulose was also significantly reduced with its evaporation during the annealing process. Therefore, both the crystallinity improvement of the CISe and the evaporation of the ethyl cellulose may contribute to the improved XRD peaks. As shown in figure 4(*a*), the sample annealed at 600 °C shows significantly improved crystallinity of the CISe, thus the 600 °C was chosen as annealing temperature in the following experiments.

Figure 4(*b*) demonstrates the XRD pattern of samples prepared at various annealing times (annealing temperature is 600 °C). The diffraction peaks of the sample annealed for 5 min are relatively weak and broad, whereas, they become sharp and strong when the annealing time is prolonged to 10 min or more. However, when the annealing time is further increased to 15 or 20 min, the XRD peaks do not show big change compared with that of 10 min.

3.3.2. UV–vis–IR analysis. We also investigated the optical property of the ethyl cellulose/CISe composite absorber layer by UV–vis–IR absorption spectra. As shown in figure 5 (samples annealed at 400 °C and 500 °C are also included): the as-deposited sample does not show clear absorption edge, possibly because of the amorphous nature of the as-synthesized CISe powder and the large amount of viscosity controlling agent, whereas all the annealed samples show clear absorption edges. This indicates the annealing process can effectively improve the crystallinity of the CISe and reduce the amount of viscosity controlling agent. However, in the long wavelength range ($\geqslant$1300 nm), the light absorption of the samples annealed at 600 °C for 15 min is rather high compared with that of the samples annealed at 400 or 500 °C for 15 min, which may be due to the inter-bandgap defects existing in the high-temperature annealed composite absorber layers. The light absorption of the samples annealed at 600 °C for 20 min changes back to relatively flat at the long wavelength range ($\geqslant$1300 nm) compared with that of the sample annealed at 600 °C for 15 min. This indicates the inter-bandgap defects that exist in the sample annealed for 15 min may have become the main component of the sample anneal for 20 min.

In addition, using a simple bandgap value (E_g) measurement method of $E_g = h \times C/\lambda$ (h is Planck's constant, C is the speed of light and λ is the absorption cutoff wavelength that can be obtained from the absorption spectra), the calculated bandgap values of the samples annealed at (400 °C, 15 min), (500 °C, 15 min), (600 °C, 5 min), (600 °C, 10 min), (600 °C, 15 min) and (600 °C, 20 min) are 0.86 eV, 0.94 eV, 0.88 eV, 1.00 eV, 1.01 eV and 0.98 eV, respectively. The bandgap value generally increases as the annealing temperature and/or annealing time increases. When the annealing condition is (600 °C, 15 min), the bandgap value is 1.01 eV, which is in good agreement with the reported value of 1.02 eV [19]. The bandgap value is decreased to 0.98 eV when the annealing time is increased to 20 min, which indicates the element molar ratio of CISe in the sample annealed for 20 min may have significantly deviated its standard element molar ratio ($CuInSe_2$, Cu : In : Se = 1 : 1 : 2). This deterioration may be due to the significant evaporation of In and Se atoms from the CISe during the annealing process at high temperature for long time [20–22], as both of their melting points are low (In, 150 °C; Se, 220 °C). Therefore, from the XRD and UV–vis–IR reults, the optimal annealing condition could be (600 °C, 15 min).

3.3.3. J–V analysis. The electronic property of the ethyl cellulose/CISe composite absorber layer was measured by employing a simple superstrate solar cell structure of Mo/absorber layer/In_2S_3/TiO_2/FTO glass. Figure 7 shows the J–V characteristics of the samples prepared at 600 °C for various annealing times (solar cell parameters are summarized in table 1). As depicted in figure 7, the as-deposited absorber layer (0 min) does not show any photovoltaic effect, which may be due to the large amount of insulating ethyl cellulose that totally blocks down the electron transmission in the as-deposited absorber layer. However, the annealed absorber layers turn out obvious photovoltaic behaviour. The J_{sc} of the solar cell continuously increases as the annealing time increases from 5 to 10 and 15 min. However, it decreases as the annealing time is further increased to 20 min. The increased J_{sc} may be due to the improved micro-structural and macro-morphologic properties of the ethyl cellulose/CISe composite absorber layer. The crystallinity of the CISe was improved with the increased annealing time, which reduces the carrier recombination in the bulk CISe. In addition, the amount of the ethyl cellulose could also become smaller with the increased annealing time, which reduces the obstruction of the electron

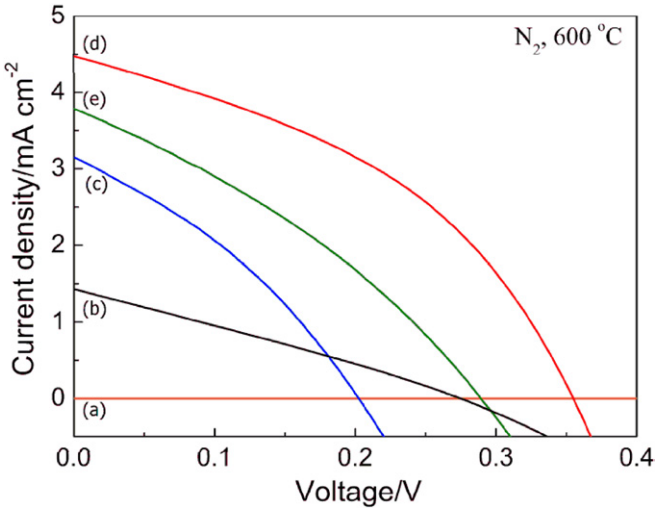

Figure 7. J–V characteristics of composite absorber layers prepared in N_2 ambience at 600 °C for (a) 0 min; (b) 5 min; (c) 10 min; (d) 15 min; (e) 20 min.

Table 1. Solar cell parameters summarized from figure 7.

Annealing time (min)	J_{sc} (mA cm^{-2})	V_{oc} (V)	FF	Efficiency (%)
0	0	0.20	0.38	0
5	1.43	0.27	0.27	0.11
10	3.15	0.20	0.33	0.21
15	4.48	0.36	0.41	0.65
20	3.79	0.29	0.33	0.36

transmission. Thus both of these improvements can contribute to the increased J_{sc}. However, overlong annealing (20 min) caused the CISe to significantly deviate from its standard element molar ratio, which resulted in the reduced J_{sc}. These results are consistent with those from XRD and UV–vis–IR. Table 1 indicates the J_{sc}, V_{oc}, FF and efficiency of the best solar cell are 4.48 mA cm^{-2}, 360 mV, 0.41 and 0.65%, respectively.

From the above discussion, the photovoltaic behaviour of the composite absorber layer may be dominated by the micro-structural and macro-morphologic properties of the ethyl cellulose/CISe composite absorber layer. The insulating ethyl cellulose is generally considered as a barrier for the electron transmission in the composite absorber layer. The CISe particles, which tightly connect to each other, may act as both absorber material and transmission path of the generated electron. Various annealing conditions change both the micro-structural and macro-morphologic properties of the composite absorber layer, and hence affect its photovoltaic property.

4. Conclusion

A printed ethyl cellulose/CISe composite absorber layer was reported and its photovoltaic property was studied. The as-deposited absorber layer contains a large amount of insulting ethyl cellulose which totally blocks down the electron transmission between the CISe particles. The annealing process can improve the crystallinity of the CISe and reduce the amount of ethyl cellulose, and thus it can facilitate the electron transmission through the CISe particles. However, overlong annealing may cause the CISe to significantly deviate from its standard element molar ratio. The composite absorber layer showed photovoltaic properties of $J_{sc} = 4.48$ mA cm^{-2}, $V_{oc} = 360$ mV, FF $= 0.41$ and efficiency $= 0.65\%$, respectively. In order to better understand the photovoltaic effect, a more detailed study of electron transmission and recombination in the composite absorber layer is under way. Such a study may offer new insight into printed absorber layer from polymer-based paste.

Acknowledgment

This work was supported by the Shanghai Committee of Science and Technology, China (Grant No 10540500700).

References

[1] Jackson P, Hariskos D, Lotter E, Paetel S, Wuerz R, Menner R, Wischmann W and Powalla M 2011 *Prog. Photovolt.: Res. Appl.* doi:10.1002/pip.1078
[2] Repins I, Contreras M A, Egaas B, DeHart C, Scharf J, Perkins C L, To B and Noufi R 2008 *Prog. Photovolt.: Res. Appl.* **16** 235
[3] Chenene M L and Alberts V 2003 *J. Phys. D: Appl. Phys.* **36** 56
[4] Kapur V K, Bansal A, Le P and Asensio O I 2003 *Thin Solid Films* **431** 53
[5] Kaelin M, Rudmann D, Kurdesau F, Zogg H, Meyer T and Tiwari A N 2005 *Thin Solid Films* **480–481** 486
[6] Ahn S J, Kim K H and Yoon K H 2008 *Colloids Surf.* A **313–314** 171
[7] Wada T, Matsuo Y, Nomura S, Nakamura Y, Miyamura A, Chiba Y, Yamada A and Konagai M 2006 *Phys. Status Solidi* a **203** 2593
[8] Guo Q, Ford G M, Yang W C, Walker B C, Stach E A, Hillhouse H W and Agrawal R 2010 *J. Am. Chem. Soc.* **132** 17384
[9] Mitzi D B, Yuan M, Liu W, Kellock A J, Chey S J, Deline V and Schrott A G 2008 *Adv. Mater.* **20** 3657
[10] Oja I, Nanu M, Katerski A, Krunks M, Mere A, Raudoja J and Goossens A 2005 *Thin Solid Films* **480–481** 82
[11] Dale P J, Samantilleke A P, Zoppi G, Forbes I and Peter L M 2008 *J. Phys. D: Appl. Phys.* **41** 085105
[12] Scragga J J, Daleb P J and Peter L M 2008 *Electrochem. Commun.* **10** 639
[13] Park J W, Choi Y W, Lee E, Joo O S, Yoon S and Min B K 2009 *J. Cryst. Growth* **311** 2621
[14] Haug V, Quintilla A, Klugius I and Ahlswede E 2011 *Thin Solid Films* **519** 7464
[15] Ahn S J, Kim C W, Yun J H, Gwak J, Jeong S, Ryu B H and Yoon K H 2010 *J. Phys. Chem.* C **114** 8108
[16] Kavan L and Gratzel M 1995 *Electrochim. Acta* **40** 643
[17] John T T, Bini S, Kashiwaba Y, Abe T, Yasuhiro Y, Kartha C S and Vijayakumar K P 2003 *Semicond. Sci. Technol.* **18** 491
[18] Yadav S and Srivastava A K 2002 *J. Polym. Res.* **9** 265
[19] Grindle S P, Clark A H, Rezaie-Serej S, Falconer E, McNeily J and Kazmerski L L 1980 *J. Appl. Phys.* **51** 5464
[20] Deepa K G, Kumar P M R, Kartha C S and Vijayakumar K P 2006 *Sol. Energy Mater. Sol. Cells* **90** 3481
[21] Valdés M H and Vázquez M 2011 *Electrochim. Acta* **56** 6866
[22] Shah N M, Panchal C J, Kheraj V A, Ray J R and Desai M S 2009 *Sol. Energy* **83** 753